Published in final edited form as:

J Immunol. 2020 November 15; 205(10): 2778–2785. doi:10.4049/jimmunol.2000244.

RIPK3 promotes *Mefv* expression and pyrin inflammasome activation via modulation of mTOR signaling

Deepika Sharma[1], **Ankit Malik**[1], **Arjun Balakrishnan**[1], **R.K. Subbarao Malireddi**[1], **Thirumala-Devi Kanneganti**[1,*]

[1]Department of Immunology, St. Jude Children's Research Hospital, Memphis, TN, 38105, USA

Abstract

Mutations in *MEFV*, the gene encoding pyrin in humans, are associated with the autoinflammatory disorder familial Mediterranean fever (FMF). Pyrin is an innate sensor that assembles into an inflammasome complex in response to Rho-modifying toxins, including *Clostridium difficile* toxins A and B. Cell death pathways have been shown to intersect with and modulate inflammasome activation, thereby affecting host defense. Using bone marrow-derived macrophages and a murine model of peritonitis, we show here that receptor-interacting protein kinase 3 (RIPK3) impacts pyrin inflammasome activation independent of its role in necroptosis. RIPK3 was instead required for transcriptional upregulation of *Mefv* through negative control of the mechanistic target of rapamycin (mTOR) pathway and independent of alterations in MAPK and NF-κB signaling. RIPK3 did not affect pyrin dephosphorylation associated with inflammasome activation. We further demonstrate that inhibition of mTOR is sufficient to promote *Mefv* expression and pyrin inflammasome activation, highlighting the crosstalk between the mTOR pathway and regulation of the pyrin inflammasome. Our study reveals a novel interaction between molecules involved in cell death and mTOR pathways to regulate the pyrin inflammasome which can be harnessed for therapeutic interventions.

Keywords

pyrin; *Mefv*; RIPK3; mTOR; inflammasome; cell death; *Clostridium difficile*; TcdB; innate immunity

INTRODUCTION

Mutations in the pyrin-encoding gene *MEFV* are associated with familial Mediterranean fever (FMF), an autoinflammatory disorder (1, 2). Pyrin has been recognized as an innate sensor that assembles an inflammasome complex with apoptosis-associated speck-like protein containing a caspase recruitment domain (ASC) and caspase-1 in response to Rho

[*]**Correspondence to:** Thirumala-Devi Kanneganti, Department of Immunology, St. Jude Children's Research Hospital, MS #351, 262 Danny Thomas Place, Memphis TN 38105-3678, Tel: (901) 595-3634; Fax. (901) 595-5766. Thirumala-Devi.Kanneganti@StJude.org.
Author Contributions: Conceptualization, D.S., T.-D.K.; Methodology, D.S., A.M., A.B.; Investigation and Analysis, D.S., A.M., A.B., and R.K.S.M.; Writing – Original Draft, D.S. and R.K.S.M.; Writing – Review & Editing, D.S., A.M., R.K.S.M. and T.-D.K.; Funding Acquisition, T.-D.K.; Resources, T.-D.K.; Supervision, T.-D.K.

Conflict of Interest Statement: The authors declare no conflict of interest.

modifications induced by bacterial toxins (3–5). Rho modification is a common mechanism employed by bacteria to hijack host cytoskeleton and subvert effector responses (6). The ability of the host cell to identify this subversion is essential for an effective innate immune response.

Clostridium difficile is an enteric pathogen whose prevalence has been increasing due to microbial dysbiosis induced by prolonged antibiotic use and compromised immune status (7, 8). *C. difficile* produces two large exotoxins, toxin A (TcdA) and toxin B (TcdB) that glycosylate and inactivate Rho, thereby instigating the anti-pathogen host response (9). Toxin production by *C. difficile* is an integral part of its pathogenesis, and several treatment regimens target toxin neutralization or absorption to alleviate the clinical symptoms (8–11). *C. difficile* mutants that lack Rho glycosylating toxins have significantly reduced pathology, and challenge with toxin alone is sufficient to promote pathology in various animal models (9, 12, 13). These findings highlight the importance of the toxin-induced immune response in *C. difficile* pathogenesis and the need to investigate the underpinnings of toxin-mediated pathology.

TcdB-mediated Rho inactivation was recently shown to activate the pyrin inflammasome. This makes pyrin a unique innate sensor because it recognizes a bacteria-induced host modification instead of a molecular pattern associated with pathogens (3). Pyrin activation has diverse roles in host defense, and its dysregulation can be detrimental during infectious or sterile insults. Pyrin inflammasome activation contributes to inflammation and pathology in a murine model of FMF (14, 15), promotes host defense in response to *Burkholderia cenocepacia* infection (5, 16), and is required for maintenance of epithelial barrier integrity during mucosal injury (17). Furthermore, inflammasome activation in general has been shown to be detrimental to the host during *C. difficile* infection and can modulate various aspects of resulting inflammation (18). While Rho modifications play a key role in activating the pyrin inflammasome, little is known about the details of the molecular pathways involved in this process.

To fill this gap in knowledge, we have investigated the pathways involved in pyrin inflammasome activation and previously identified a role for TNF signaling (19). TNF signaling promotes major cellular pathways, including inflammation, cell survival, and cell death (20). Receptor-interacting protein kinase 1 (RIPK1) and RIPK3 are critical components of a signaling network downstream of the TNF receptor. The fate of a cell in response to a TNF stimulus varies between NF-κB–induced cell survival, Fas-associated death domain /caspase-8–induced apoptotic cell death, and mixed lineage kinase domain-like pseudokinase (MLKL)-induced necroptotic cell death (21). We sought to investigate the impact of pathways downstream of TNF signaling on pyrin inflammasome activation.

Here, we demonstrate that RIPK3 is involved in pyrin inflammasome activation, and this inflammasome activation is independent of the necroptotic and apoptotic cell death pathways. We further demonstrate that RIPK3 modulates the mechanistic target of rapamycin (mTOR) pathway to regulate *Mefv* expression and pyrin inflammasome activation. This study highlights the impact of RIPK3 and mTOR modulation on pyrin inflammasome activation.

METHODS

Mice

Pyrin$^{-/-}$ (22), *Casp1*$^{-/-}$ (23), *Tnf*$^{-/-}$ (24), *Nlrp3*$^{-/-}$ (25), *Ripk3*$^{-/-}$ (26), *Mlkl*$^{-/-}$ (27), *Casp3*$^{-/-}$ (28), *Casp7*$^{-/-}$ (29), *Myd88*$^{-/-}$ (30) and *Trif*$^{-/-}$ (31) mice have been previously described. Mice were maintained in a specific pathogen-free facility, and animal studies were approved by St. Jude Children's Research Hospital Committee on the Use and Care of Animals.

Toxin preparation

Clostridium difficile strain r20291 AB- and AB+ strains were provided by Dr. N. Minton, and toxin was prepared as described previously (9). Briefly, *C. difficile* strain r20291 (AB- and AB+) was cultured in tryptone-yeast extract media for 24 hours in an anaerobic chamber at 37°C. Cultures were diluted to an OD of 1 (corresponds to 2×10^7 CFU/mL), and spun down, and the supernatant was sterilized using 0.22 μM filters. Supernatant prepared from toxin-positive strain was used to stimulate BMDMs at a 1:5 dilution. This stimulation is referred to as "*C. difficile* toxin" stimulation. Supernatant prepared from toxin-negative strain is referred to as "control" stimulation and included in all experiments with crude *C. difficile* toxin as the stimulus.

Cell culture and stimulation

BMDMs were generated as previously described (32). For pyrin inflammasome activation, cells were resuspended in Opti-MEM (Gibco) and stimulated with *C. difficile* supernatant (AB- [control] or AB+) for 12–16 hours. Alternately, cells were stimulated with 0.2 μg/mL TcdB (List Biologicals) or medium for 6–8 hours. For mTOR inhibition, 1 μM rapamycin (InvivoGen), 200 nM torin1 (Selleckchem), or 200 nM PP242 (Selleckchem) was added to cells 30 minutes prior to stimulation with toxins.

Light microscopy and histology

BMDMs differentiated from specific mouse strains were seeded in 12-well cell culture plates and treated with the indicated stimuli for pre-determined amounts of time. Image-based light microscopy data were collected using an Olympus CKX41 microscope with a 40× objective lens. The acquired data were digitally analysed using the INFINITY ANALYZE Software (Lumenera Corporation).

IncuCyte cell death analysis

Cell death was carried out using a 2-color IncuCyte Zoom in incubator imaging system (Essen Biosciences). BMDMs were sub-cultured at 1.0×10^6 cells/well in treated 12-well cell culture plates and were treated with different experimental conditions inducing cell death in the presence of 100 nM of the cell-impermeable DNA binding fluorescent dye Sytox green (Life Technologies, S7020). Loss of membrane integrity in the dying cells results in uptake and positive staining for the Sytox green dye. Several images at different timepoints were collected using a 20× objective and analysed using the IncuCyte S3 software, which allows precise quantification of the number of Sytox green-positive dead

cells present in each image. The number of dead cells for each of the stimulations and mouse strains was exported for quantitative analysis of the total cell death.

Immunoblot analysis

BMDM cell lysates and supernatants were combined in caspase lysis buffer (protease inhibitors, phosphatase inhibitors, 10% NP40, and 25 mM DTT) and boiled in sodium dodecyl sulfate (SDS) sample buffer for western blot analysis. These lysates were used for analysis of caspase processing. For signaling analysis, BMDMs were lysed in complete RIPA buffer (containing protease inhibitors and phosphatase inhibitors [Calbiochem, Massachusetts]), and boiled in SDS sample buffer for western blot analysis. Pyrin phosphorylation status was assessed as previously described (33) using Mn^{2+}-based phospho-tag gel analysis (Fujifilm Wako Chemicals). Proteins were separated by electrophoresis using 6–12% polyacrylamide gels. Following electrophoresis, proteins were transferred to PVDF membranes (Millipore), blocked in 5% skim milk to reduce non-specific binding, and probed with primary antibodies. Membranes were then washed and incubated with appropriate horseradish peroxide (HRP)-conjugated secondary antibody (1:5000, Jackson Immuno Research Laboratories). Proteins were visualized using the Luminata Forte Western HRP substrate (Millipore). The primary antibody used for caspase processing analysis was anti–caspase-1 (1:3000, AG-20B-0042-C100, Adipogen). Antibodies used for signaling immunoblotting were anti-phospho (p)-ERK1/2 (#9101, 1:1000, Cell Signaling Technologies), anti-total (t)-ERK1/2 (#9102, 1:1000, Cell Signaling Technologies), anti–p-IκBα (#2859, 1:1000, Cell Signaling Technologies), anti–t-IκBα (#9242, 1:1000, Cell Signaling Technologies), anti–p-p38 (#9211, 1:1000, Cell Signaling Technologies), anti–p-JNK (#9251, 1:1000, Cell Signaling Technologies), anti–p-pyrin S241 (ab200420, 1:1000, Abcam), anti–pyrin (ab195975, 1:1000, Abcam), anti–14–3-3 (#8312, 1:1000, Cell Signaling Technologies), anti–p-mTOR S2481 (#2974, 1:1000, Cell Signaling Technologies), anti–p-mTOR S2448 (#2971, 1:1000, Cell Signaling Technologies), anti–p-GSK3β (#5558, 1:1000, Cell Signaling Technologies), anti–p-S6K (#9205, 1:1000, Cell Signaling Technologies), and anti–p-S6 (#4856, 1:1000, Cell Signaling Technologies). Anti-GAPDH (#5174, 1:1000, Cell Signaling Technologies) was used as a control.

Real-time (RT-PCR) analysis

RNA was extracted using TRIzol (Thermo Fisher Scientific) according to the manufacturer's instructions. The isolated RNA was reverse-transcribed using the First-Strand cDNA Synthesis Kit (Applied Biosystems), and real-time quantitative PCR was performed using 2× SYBR Green (Applied Biosystems) using appropriate primers on ABI 7500 RT-PCR instrument. RT-PCR primer sequences are TNF: forward CATCTTCTCAAAATTCGAGTGACAA, reverse TGGGAGTAGACAAGGTACAACCC; pyrin: forward TCATCTGCTAAACACCCTGGA, reverse GGGATCTTAGAGTGGC CCTTC; and forward primer-2 AGGCTTCAAGGACTTTACAACAA, reverse primer-2 TCATGCGAATGAGACTCCCA; and GAPDH: forward CGTCCCGTAGACAAAATGGT, reverse TTGA TGGCAACAATCTCCAC.

LDH assay

LDH assay (Promega, Madison, WI) was carried out as per the manufacturer's instructions. Briefly, cell culture supernatants were incubated with the substrate at 37°C for 15 minutes, and the end point colorimetric assay was read at 450 nM. A standard curve was generated using cellular lysate of known density and percent cell death extrapolated using the curve.

Toxin peritonitis model

Toxin was prepared as described above, and 1 mL (control or toxin) was injected intraperitoneally into gender-matched mice at 8–10 weeks of age. Four hours post injection, blood was harvested through cardiac puncture, and serum was isolated for cytokine analysis.

ELISA

Cytokines in the serum and cell culture supernatants were measured by ELISA, according to the manufacturers' instructions. The IL-18 and multiplex ELISA kits were obtained from eBiosciences and Millipore, respectively.

Statistics

All statistical analysis was performed using Prism v6.0 software. Student's t-test, one-way ANOVA followed by Fischer's least significance difference (LSD), or Kruskal-Wallis followed by Dunn's post-test was used for statistical analysis as indicated. P values less than 0.05 were considered significant.

RESULTS

RIPK3 is required for efficient activation of the pyrin inflammasome

The pyrin inflammasome is activated in response to purified *C. difficile* toxins TcdA and TcdB in bone marrow-derived macrophages (BMDMs) (3, 33), and we have previously shown that loss of TNF leads to reduced caspase-1 cleavage, IL-18 release, and pyroptotic cell death in response to pyrin inflammasome activation by *C. difficile* toxin (19). Here, we went on to test whether loss of major components of the TNF signaling pathway affected pyrin inflammasome activation. Wild type (WT) BMDMs stimulated with *C. difficile* toxin underwent pyrin inflammasome activation, indicated by pyrin-dependent caspase-1 cleavage and IL-18 maturation (Fig. 1A, 1B), and pyroptotic cell death, indicated by LDH release and membrane permeability (Fig. 1C–1E). Loss of RIPK3 resulted in a reduction in pyrin inflammasome activation (Fig. 1A–1E), demonstrating that RIPK3 promotes pyrin inflammasome activation in response to *C. difficile* toxin.

RIPK3 controls pyrin inflammasome activation independent of necroptosis

RIPK3 has important roles in regulating inflammatory signaling and promoting necroptosis (34). We therefore tested whether disrupting necroptosis impacted pyrin inflammasome activation. Loss of MLKL, the necroptosis executioner downstream of RIPK3, did not affect pyrin inflammasome activation, as levels of caspase-1 cleavage, IL-18 release, and pyroptotic cell death were similar between WT and *Mlkl*$^{-/-}$ BMDMs treated with *C. difficile* toxin (Fig. 2A–2D). This suggests that RIPK3 promotes pyrin inflammasome activation

independent of its role in necroptosis. Similarly, the loss of apoptosis executioners, caspase-3 and −7 also did not affect levels of caspase-1 cleavage, IL-18 release, and pyroptotic cell death in response to treatment with *C. difficile* toxin (Fig. 2E–2H). These data demonstrate that the function of RIPK3 in promoting pyrin inflammasome activation is independent of its role in necroptosis and independent of apoptosis.

RIPK3 controls pyrin expression but not pyrin dephosphorylation

Supernatants obtained from *C. difficile* cultures contain various pathogen-associated molecular pattern (PAMPs) that can modulate inflammatory signaling (35, 36). The pyrin inflammasome has been previously shown to be primed by TLR signaling (22). We assessed the role of RIPK3 in the activation of inflammatory signaling pathways downstream of TLRs including MAPK and NF-κB. *C. difficile* toxin stimuli promoted the phosphorylation of ERK, p38, JNK, and IκBα, demonstrating that these pathways were activated in response to the bacterial components (including toxin) (Fig. 3A). The loss of RIPK3 did not affect the activation of MAPK and NF-κB pathways (Fig. 3A). Pyrin expression, on the other hand, was notably reduced in the absence of RIPK3 (Fig. 3A). To test whether differential pyrin expression was caused by transcriptional regulation, we assessed the level of *Mefv* transcript in response to the stimuli. The *Mefv* transcript levels mirrored the protein expression pattern and were reduced in *Ripk3*$^{-/-}$ cells compared with WT cells, both under basal and stimulated conditions, while *Tnf* transcript levels were similar between *Ripk3*$^{-/-}$ and WT cells (Fig. 3B).

Given the relevance of the TNF-TNFR axis in pyrin activation (19) and the role of RIPK3 in TNFR signaling, we assessed the role of TLR signaling in TNF induction. TLR signaling relies on the adaptor proteins MyD88 and TRIF; we therefore tested pyrin inflammasome activation in macrophages deficient in MyD88 or TRIF. MyD88 was required for caspase-1 cleavage (Supplementary Fig. 1A), IL-18 release (Supplementary Fig. 1B), and cell death induced by *C. difficile* toxin (Supplementary Fig. 1C, D), while TRIF was dispensable (Supplementary Fig. 1A, B). We further found that MyD88, and not TRIF, was required for TNF production and *Mefv* expression in response to *C. difficile* toxin (Supplementary Fig. 1B, E, F). These data demonstrate that MyD88 is required for the TNF production that engages the RIPK3 pathway to promote pyrin activation in response to *C. difficile* toxin stimuli.

To specifically test whether pyrin inflammasome activation is independent of the signaling engaged by other PAMPs in the *C. difficile* toxin stimuli, we stimulated BMDMs with purified TcdB. Similar to the response to *C. difficile* toxin stimuli, pyrin inflammasome activation in response to purified TcdB was significantly reduced in *Ripk3*$^{-/-}$ BMDMs compared with WT BMDMs, as indicated by reduced caspase-1 cleavage, IL-18 release, and cell death (Fig. 3C, 3D, and Supplemental Fig. 2).

Recent studies have identified pyrin dephosphorylation as a critical step upstream of pyrin inflammasome activation (33, 37, 38). We therefore assessed whether pyrin dephosphorylation was affected in the absence of RIPK3. We found that the loss of RIPK3 reduced pyrin expression but did not affect pyrin dephosphorylation (Fig. 3E). Overall these data suggest that the modulation of pyrin inflammasome activation by RIPK3 occurs at the

level of *Mefv* transcript and protein expression and is independent of MAPK and NF-κB signaling and pyrin dephosphorylation.

Loss of RIPK3 enhances mTOR signaling, which in turn suppresses *Mefv* expression and pyrin inflammasome activation

In addition to MAPK and NF-κB signaling, *Mefv* expression is regulated by the mTOR (39) and PI3K pathways (40). We assessed mTOR activation in BMDMs following *C. difficile* toxin stimuli exposure. We observed increased phosphorylation of mTOR, GSK3β, and downstream targets S6K and S6 in the absence of RIPK3 (Fig. 4A). These data demonstrate that RIPK3 restricts mTOR activation following *C. difficile* toxin stimuli. To assess whether mTOR activation modulates pyrin inflammasome activation, we inhibited mTOR activation using rapamycin treatment during stimulation with *C. difficile* toxin (Fig. 4B). Treatment with rapamycin increased the amount of caspase-1 cleavage and IL-18 released in response to the *C. difficile* toxin stimuli (Fig. 4C, 4D). Additionally, rapamycin treatment increased *Mefv* transcript levels independent of MAPK or NF-κB modulation (Supplemental Fig. 3A, 3B). To confirm that mTOR inhibition specifically led to pyrin inflammasome activation in response to *C. difficile* toxin stimuli, we tested the effect of rapamycin on *C. difficile* toxin-induced inflammasome activation in *Nlrp3*$^{-/-}$ BMDMs (41). We observed that rapamycin promoted *C. difficile* toxin-induced inflammasome activation that was independent of NLRP3 and dependent on pyrin (Supplemental Fig. 3C, 3D).

To confirm the role of mTOR signaling in pyrin inflammasome activation, we also tested the effect of mTOR inhibitors PP242 and torin1 on pyrin inflammasome activation. Similar to the effects of rapamycin treatment, treatment with PP242 and torin1 promoted pyrin inflammasome activation in response to *C. difficile* toxin stimuli (Fig. 4E, 4F). In line with the observed pyrin inflammasome activation, mTOR inhibition also promoted IL-1β release, but it did not consistently affect release of the non-inflammasome cytokines TNF and IL-6 (Supplemental Fig. 3E). Pyrin inflammasome activation was promoted in response to mTOR inhibition even upon stimulation with the purified toxin, TcdB (Supplemental Fig. 3F). Overall, these data establish an inverse correlation between the mTOR and pyrin inflammasome activation, demonstrating that negative regulation of mTOR signaling by RIPK3 can regulate *Mefv* expression and pyrin inflammasome activation.

RIPK3 promotes pyrin inflammasome activation in a peritonitis model

To test the *in vivo* relevance of these findings, we injected supernatant derived from *C. difficile* cultures (toxin-negative *C. difficile*, and toxin-positive *C. difficile*) into the mouse peritoneum and assessed inflammasome activation. Peritonitis as a model allows us to specifically address the toxin-induced innate inflammasome response independent of alterations observed in the adaptive immune system (42–44). Similar to our *in vitro* data, *C. difficile* toxin promoted pyrin- and caspase-1–mediated IL-18 release, suggesting that the toxin activates the pyrin inflammasome and promotes systemic IL-18 release in the peritonitis model (Fig. 5A). *C. difficile* toxin stimuli (irrespective of toxin status) also induced production of the inflammatory mediators, TNF and KC that, as expected, did not rely on inflammasome activation (Fig. 5A). Genetic deletion of TNF or RIPK3 reduced IL-18 release in response to the toxin stimuli, highlighting the significance of this signaling

axis in pyrin inflammasome activation (Fig. 5B). These data demonstrate that RIPK3 plays an important role in promoting activation of the pyrin inflammasome.

DISCUSSION

Our observations demonstrate a critical role for RIPK3 in *Mefv* expression and pyrin inflammasome activation. RIPK3 promotes *Mefv* expression downstream of TNF production. Neither RIPK3- and MLKL-mediated necroptosis nor caspase-3– or −7–mediated apoptosis was involved in the regulation of the pyrin inflammasome. RIPK3 was instead involved in transcriptional regulation of *Mefv* via negative control of mTOR signaling, and inhibition of mTOR activity is sufficient to upregulate *Mefv* expression and pyrin inflammasome activation. The regulation of *Mefv* expression by the RIPK3-mTOR axis could involve epigenetic control, mRNA stability, or miRNA mediated control; these are interesting topics for further research. Overall these data identify a novel regulatory mechanism for pyrin inflammasome activation.

Pyrin inflammasome activation is modulated through Rho-mediated pyrin phosphorylation and binding to 14–3-3 proteins (16, 33, 37, 38). Levels of 14–3-3 expression, Rho-mediated pyrin phosphorylation, and toxin-induced dephosphorylation were similar between WT and *Ripk3*$^{-/-}$ cells, suggesting that these factors do not contribute to the differential pyrin inflammasome activation observed in RIPK3-deficient cells. *Mefv* expression, both basal and stimulation-induced, was modulated by RIPK3 and inversely correlated with the status of mTOR activity. This observation is similar to the increased pyrin expression in cells lacking PI3K catalytic p110δ subunit (40). Our findings demonstrate that RIPK3 promotes *Mefv* expression and inflammasome activation in response to *C. difficile* toxin.

RIPK3 promotes inflammation independent of MLKL-mediated necroptosis in various settings (45–48). We similarly observed that the role of RIPK3 in the regulation of the pyrin inflammasome was independent of its role in necroptosis or inflammatory signaling and instead relied on regulation of the mTOR pathway. RIPK3-mediated necroptosis is mediated by mTOR-AKT activation (49), suggesting that RIPK3 promotes mTOR activation in response to necroptotic stimuli. However, we observed increased mTOR activation in *Ripk3*$^{-/-}$ BMDMs both at baseline and in response to *C. difficile* toxin.

In addition to the impact of mTOR on pyroptosis and the pyrin inflammasome shown here, mTOR can also influence other forms of cell death, including apoptosis (50, 51) and necroptosis (49, 52). Additionally, mTORC1 activation promotes NLRP3 inflammasome activation (53), and rapamycin limits NLRP3 inflammasome activation in response to alum and viral infections (54). This is in contrast to the role of mTOR signaling in pyrin inflammasome activation. This contrasting regulatory function of mTOR on the two inflammasomes might provide the host with a competitive advantage in cases where bacteria or other pathogenic agents actively subvert the mTOR pathway.

It was recently shown that intestinal cell death early during *C. difficile* infection is protective during self-limiting pseudomembranous colitis and proceeds independent of the pyrin inflammasome (55). However, inflammasome activation and inflammasome-dependent

IL-1 signaling have been shown to be deleterious in toxin-mediated intestinal pathology (18). Thus, pyrin activation and downstream IL-1 signaling could, under certain conditions, impact *C. difficile*-induced pathology.

Overall, our data identified RIPK3 as a critical regulator of *Mefv* expression and the pyrin inflammasome via modulation of the mTOR pathway. The regulation of the pyrin inflammasome by molecules involved in cellular functions of cell death and metabolism highlights the significance of the interplay between these pathways during inflammation. Dysregulation of the pyrin inflammasome is associated with autoinflammatory disorders and impaired host defense following infectious or sterile insults. Defining the molecular mechanisms involved in pyrin inflammasome activation is therefore critical to understanding the etiology of, and identifying therapeutic targets for, the treatment of associated inflammatory diseases.

Supplementary Material

Refer to Web version on PubMed Central for supplementary material.

ACKNOWLEDGEMENTS

We thank Dr. Nigel Minton (University of Nottingham) and Dr. William A. Petri, Jr., (University of Virginia) for providing the *C. difficile* strains. We also thank Amanda Burton for technical assistance and Drs. Teneema Kuriakose, Parimal Samir, and Rebecca Tweedell for their valuable input in editing the manuscript.

This study was supported by grants from the US National Institutes of Health (AR056296, CA253095, AI101935 and AI124346) and the American Lebanese Syrian Associated Charities to T.D.-K.

REFERENCES

1. Bernot A CC, Dasilva C, Devaud C, Petit JL, Caloustian C, Cruaud C, Samson D, Pulcini F, Weissenbach J,R, Notanicola C, Domingo C, Rozenbaum M, Benchetrit E, Topaloglu R, Dewalle M, Dross C, Hadjari P, Dupont M, Demaille J, Touitou I, Smaoui N, Nedelec B, Méry JP, Chaabouni H, Delpech M, Grateau G. 1997. A candidate gene for familial Mediterranean fever. Nat Genet 17: 25–31. [PubMed: 9288094]
2. Consortium*, T. I. F. 1997. Ancient missense mutations in a new member of the RoRet gene family are likely to cause familial Mediterranean fever. The International FMF Consortium. Cell 90: 797–807. [PubMed: 9288758]
3. Xu H, Yang J, Gao W, Li L, Li P, Zhang L, Gong Y-N, Peng X, Xi JJ, Chen S, Wang F, and Shao F. 2014. Innate immune sensing of bacterial modifications of Rho GTPases by the Pyrin inflammasome. Nature 513: 237–241. [PubMed: 24919149]
4. Gavrilin MA, Mitra S, Seshadri S, Nateri J, Berhe F, Hall MW, and Wewers MD. 2009. Pyrin critical to macrophage IL-1beta response to Francisella challenge. J Immunol 182: 7982–7989. [PubMed: 19494323]
5. Gavrilin MA, Abdelaziz DH, Mostafa M, Abdulrahman BA, Grandhi J, Akhter A, Abu Khweek A, Aubert DF, Valvano MA, Wewers MD, and Amer AO. 2012. Activation of the pyrin inflammasome by intracellular Burkholderia cenocepacia. J Immunol 188: 3469–3477. [PubMed: 22368275]
6. Haglund CM, and Welch MD. 2011. Pathogens and polymers: microbe-host interactions illuminate the cytoskeleton. J Cell Biol 195: 7–17. [PubMed: 21969466]
7. Britton RA, and Young VB. 2014. Role of the intestinal microbiota in resistance to colonization by Clostridium difficile. Gastroenterology 146: 1547–1553. [PubMed: 24503131]
8. Abt MC, McKenney PT, and Pamer EG. 2016. Clostridium difficile colitis: pathogenesis and host defence. Nat Rev Microbiol 14: 609–620. [PubMed: 27573580]

9. Kuehne SA, Collery MM, Kelly ML, Cartman ST, Cockayne A, and Minton NP. 2014. Importance of Toxin A, Toxin B, and CDT in Virulence of an Epidemic Clostridium difficile Strain. The Journal of Infectious Diseases 209: 83–86. [PubMed: 23935202]
10. Lyras D, O'Connor JR, Howarth PM, Sambol SP, Carter GP, Phumoonna T, Poon R, Adams V, Vedantam G, Johnson S, Gerding DN, and Rood JI. 2009. Toxin B is essential for virulence of Clostridium difficile. Nature 458: 1176–1179. [PubMed: 19252482]
11. Kuehne SA, Cartman ST, Heap JT, Kelly ML, Cockayne A, and Minton NP. 2010. The role of toxin A and toxin B in Clostridium difficile infection. Nature 467: 711–713. [PubMed: 20844489]
12. Carter GP, Chakravorty A, Pham Nguyen TA, Mileto S, Schreiber F, Li L, Howarth P, Clare S, Cunningham B, Sambol SP, Cheknis A, Figueroa I, Johnson S, Gerding D, Rood JI, Dougan G, Lawley TD, and Lyras D. 2015. Defining the Roles of TcdA and TcdB in Localized Gastrointestinal Disease, Systemic Organ Damage, and the Host Response during Clostridium difficile Infections. MBio 6: e00551–00515. [PubMed: 26037121]
13. Hirota SA, Iablokov V, Tulk SE, Schenck LP, Becker H, Nguyen J, Al Bashir S, Dingle TC, Laing A, Liu J, Li Y, Bolstad J, Mulvey GL, Armstrong GD, MacNaughton WK, Muruve DA, MacDonald JA, and Beck PL. 2012. Intrarectal instillation of Clostridium difficile toxin A triggers colonic inflammation and tissue damage: development of a novel and efficient mouse model of Clostridium difficile toxin exposure. Infect Immun 80: 4474–4484. [PubMed: 23045481]
14. Sharma D, Sharma BR, Vogel P, and Kanneganti TD. 2017. IL-1beta and Caspase-1 Drive Autoinflammatory Disease Independently of IL-1alpha or Caspase-8 in a Mouse Model of Familial Mediterranean Fever. Am J Pathol 187: 236–244. [PubMed: 27998728]
15. Kanneganti A, Malireddi RKS, Saavedra PHV, Vande Walle L, Van Gorp H, Kambara H, Tillman H, Vogel P, Luo HR, Xavier RJ, Chi H, and Lamkanfi M. 2018. GSDMD is critical for autoinflammatory pathology in a mouse model of Familial Mediterranean Fever. J Exp Med 215(6): 1519–1529. [PubMed: 29793924]
16. Aubert DF, Xu H, Yang J, Shi X, Gao W, Li L, Bisaro F, Chen S, Valvano MA, and Shao F. 2016. A Burkholderia Type VI Effector Deamidates Rho GTPases to Activate the Pyrin Inflammasome and Trigger Inflammation. Cell Host Microbe 19: 664–674. [PubMed: 27133449]
17. Sharma D, Malik A, Guy CS, Karki R, Vogel P, and Kanneganti TD. 2017. Pyrin Inflammasome Regulates Tight Junction Integrity to Restrict Colitis and Tumorigenesis. Gastroenterology.
18. Ng J, Hirota SA, Gross O, Li Y, Ulke-Lemee A, Potentier MS, Schenck LP, Vilaysane A, Seamone ME, Feng H, Armstrong GD, Tschopp J, Macdonald JA, Muruve DA, and Beck PL. 2010. Clostridium difficile toxin-induced inflammation and intestinal injury are mediated by the inflammasome. Gastroenterology 139: 542–552, 552.e541–543. [PubMed: 20398664]
19. Sharma D, Malik A, Guy C, Vogel P, and Kanneganti TD. 2019. TNF/TNFR axis promotes pyrin inflammasome activation and distinctly modulates pyrin inflammasomopathy. J Clin Invest 129: 150–162. [PubMed: 30457980]
20. Oberst A, and Green DR. 2011. It cuts both ways: reconciling the dual roles of caspase 8 in cell death and survival. Nat Rev Mol Cell Biol 12: 757–763. [PubMed: 22016059]
21. Sharma D, and Kanneganti TD. 2017. Inflammatory cell death in intestinal pathologies. Immunol Rev 280: 57–73. [PubMed: 29027223]
22. Van Gorp H, Saavedra PH, de Vasconcelos NM, Van Opdenbosch N, Vande Walle L, Matusiak M, Prencipe G, Insalaco A, Van Hauwermeiren F, Demon D, Bogaert DJ, Dullaers M, De Baere E, Hochepied T, Dehoorne J, Vermaelen KY, Haerynck F, De Benedetti F, and Lamkanfi M. 2016. Familial Mediterranean fever mutations lift the obligatory requirement for microtubules in Pyrin inflammasome activation. Proc Natl Acad Sci U S A 113: 14384–14389. [PubMed: 27911804]
23. Kayagaki N, Warming S, Lamkanfi M, Vande Walle L, Louie S, Dong J, Newton K, Qu Y, Liu J, Heldens S, Zhang J, Lee WP, Roose-Girma M, and Dixit VM. 2011. Non-canonical inflammasome activation targets caspase-11. Nature 479: 117–121. [PubMed: 22002608]
24. Pasparakis M, Alexopoulou L, Episkopou V, and Kollias G. 1996. Immune and inflammatory responses in TNF alpha-deficient mice: a critical requirement for TNF alpha in the formation of primary B cell follicles, follicular dendritic cell networks and germinal centers, and in the maturation of the humoral immune response. J Exp Med 184: 1397–1411. [PubMed: 8879212]

25. Kanneganti TD, Ozoren N, Body-Malapel M, Amer A, Park JH, Franchi L, Whitfield J, Barchet W, Colonna M, Vandenabeele P, Bertin J, Coyle A, Grant EP, Akira S, and Nunez G. 2006. Bacterial RNA and small antiviral compounds activate caspase-1 through cryopyrin/Nalp3. Nature 440: 233–236. [PubMed: 16407888]
26. Newton K, Sun X, and Dixit VM. 2004. Kinase RIP3 is dispensable for normal NF-kappa Bs, signaling by the B-cell and T-cell receptors, tumor necrosis factor receptor 1, and Toll-like receptors 2 and 4. Mol Cell Biol 24: 1464–1469. [PubMed: 14749364]
27. Murphy JM, Czabotar PE, Hildebrand JM, Lucet IS, Zhang JG, Alvarez-Diaz S, Lewis R, Lalaoui N, Metcalf D, Webb AI, Young SN, Varghese LN, Tannahill GM, Hatchell EC, Majewski IJ, Okamoto T, Dobson RC, Hilton DJ, Babon JJ, Nicola NA, Strasser A, Silke J, and Alexander WS. 2013. The pseudokinase MLKL mediates necroptosis via a molecular switch mechanism. Immunity 39: 443–453. [PubMed: 24012422]
28. Zheng TS, Hunot S, Kuida K, Momoi T, Srinivasan A, Nicholson DW, Lazebnik Y, and Flavell RA. 2000. Deficiency in caspase-9 or caspase-3 induces compensatory caspase activation. Nat Med 6: 1241–1247. [PubMed: 11062535]
29. Lakhani SA, Masud A, Kuida K, Porter GA Jr., Booth CJ, Mehal WZ, Inayat I, and Flavell RA. 2006. Caspases 3 and 7: key mediators of mitochondrial events of apoptosis. Science 311: 847–851. [PubMed: 16469926]
30. Kawai T, Adachi O, Ogawa T, Takeda K, and Akira S. 1999. Unresponsiveness of MyD88-deficient mice to endotoxin. Immunity 11: 115–122. [PubMed: 10435584]
31. Yamamoto M, Sato S, Hemmi H, Hoshino K, Kaisho T, Sanjo H, Takeuchi O, Sugiyama M, Okabe M, Takeda K, and Akira S. 2003. Role of adaptor TRIF in the MyD88-independent toll-like receptor signaling pathway. Science 301: 640–643. [PubMed: 12855817]
32. Gurung P, Anand PK, Malireddi RK, Vande Walle L, Van Opdenbosch N, Dillon CP, Weinlich R, Green DR, Lamkanfi M, and Kanneganti TD. 2014. FADD and caspase-8 mediate priming and activation of the canonical and noncanonical Nlrp3 inflammasomes. J Immunol 192: 1835–1846. [PubMed: 24453255]
33. Gao W, Yang J, Liu W, Wang Y, and Shao F. 2016. Site-specific phosphorylation and microtubule dynamics control Pyrin inflammasome activation. Proc Natl Acad Sci U S A 113: E4857–4866. [PubMed: 27482109]
34. Orozco S, and Oberst A. 2017. RIPK3 in cell death and inflammation: the good, the bad, and the ugly. Immunol Rev 277: 102–112. [PubMed: 28462521]
35. Ausiello CM, Cerquetti M, Fedele G, Spensieri F, Palazzo R, Nasso M, Frezza S, and Mastrantonio P. 2006. Surface layer proteins from Clostridium difficile induce inflammatory and regulatory cytokines in human monocytes and dendritic cells. Microbes Infect 8: 2640–2646. [PubMed: 16935543]
36. Bianco M, Fedele G, Quattrini A, Spigaglia P, Barbanti F, Mastrantonio P, and Ausiello CM. 2011. Immunomodulatory activities of surface-layer proteins obtained from epidemic and hypervirulent Clostridium difficile strains. J Med Microbiol 60: 1162–1167. [PubMed: 21349985]
37. Park YH, Wood G, Kastner DL, and Chae JJ. 2016. Pyrin inflammasome activation and RhoA signaling in the autoinflammatory diseases FMF and HIDS. Nat Immunol: 914–921. [PubMed: 27270401]
38. Masters SL, Lagou V, Jeru I, Baker PJ, Van Eyck L, Parry DA, Lawless D, De Nardo D, Garcia-Perez JE, Dagley LF, Holley CL, Dooley J, Moghaddas F, Pasciuto E, Jeandel PY, Sciot R, Lyras D, Webb AI, Nicholson SE, De Somer L, van Nieuwenhove E, Ruuth-Praz J, Copin B, Cochet E, Medlej-Hashim M, Megarbane A, Schroder K, Savic S, Goris A, Amselem S, Wouters C, and Liston A. 2016. Familial autoinflammation with neutrophilic dermatosis reveals a regulatory mechanism of pyrin activation. Sci Transl Med 8: 332ra345.
39. Mitroulis I, Kourtzelis I, Kambas K, Chrysanthopoulou A, and Ritis K. 2011. Evidence for the involvement of mTOR inhibition and basal autophagy in familial Mediterranean fever phenotype. Hum Immunol 72: 135–138. [PubMed: 21081147]
40. Akula MK, Shi M, Jiang Z, Foster CE, Miao D, Li AS, Zhang X, Gavin RM, Forde SD, Germain G, Carpenter S, Rosadini CV, Gritsman K, Chae JJ, Hampton R, Silverman N, Gravallese EM, Kagan JC, Fitzgerald KA, Kastner DL, Golenbock DT, Bergo MO, and Wang D. 2016. Control

of the innate immune response by the mevalonate pathway. Nat Immunol 17: 922–929. [PubMed: 27270400]

41. Sharma D, and Kanneganti TD. 2016. The cell biology of inflammasomes: Mechanisms of inflammasome activation and regulation. J Cell Biol 213: 617–629. [PubMed: 27325789]
42. Kaiser WJ, Upton JW, Long AB, Livingston-Rosanoff D, Daley-Bauer LP, Hakem R, Caspary T, and Mocarski ES. 2011. RIP3 mediates the embryonic lethality of caspase-8-deficient mice. Nature 471: 368–372. [PubMed: 21368762]
43. Oberst A, Dillon CP, Weinlich R, McCormick LL, Fitzgerald P, Pop C, Hakem R, Salvesen GS, and Green DR. 2011. Catalytic activity of the caspase-8-FLIP(L) complex inhibits RIPK3-dependent necrosis. Nature 471: 363–367. [PubMed: 21368763]
44. Dillon CP, Oberst A, Weinlich R, Janke LJ, Kang TB, Ben-Moshe T, Mak TW, Wallach D, and Green DR. 2012. Survival function of the FADD-CASPASE-8-cFLIP(L) complex. Cell Rep 1: 401–407. [PubMed: 22675671]
45. Kuriakose T, Man SM, Malireddi RK, Karki R, Kesavardhana S, Place DE, Neale G, Vogel P, and Kanneganti TD. 2016. ZBP1/DAI is an innate sensor of influenza virus triggering the NLRP3 inflammasome and programmed cell death pathways. Sci Immunol 1.
46. Lawlor KE, Khan N, Mildenhall A, Gerlic M, Croker BA, D'Cruz AA, Hall C, Kaur Spall S, Anderton H, Masters SL, Rashidi M, Wicks IP, Alexander WS, Mitsuuchi Y, Benetatos CA, Condon SM, Wong WW, Silke J, Vaux DL, and Vince JE. 2015. RIPK3 promotes cell death and NLRP3 inflammasome activation in the absence of MLKL. Nat Commun 6: 6282. [PubMed: 25693118]
47. Newton K, Dugger DL, Maltzman A, Greve JM, Hedehus M, Martin-McNulty B, Carano RAD, Cao TC, van Bruggen N, Bernstein L, Lee WP, Wu X, DeVoss J, Zhang J, Jeet S, Peng I, McKenzie BS, Roose-Girma M, Caplazi P, Diehl L, Webster JD, and Vucic D. 2016. RIPK3 deficiency or catalytically inactive RIPK1 provides greater benefit than MLKL deficiency in mouse models of inflammation and tissue injury. Cell Death and Differentiation 23: 1565–1576. [PubMed: 27177019]
48. Najjar M, Saleh D, Zelic M, Nogusa S, Shah S, Tai A, Finger JN, Polykratis A, Gough PJ, Bertin J, Whalen M, Pasparakis M, Balachandran S, Kelliher M, Poltorak A, and Degterev A. 2016. RIPK1 and RIPK3 Kinases Promote Cell-Death-Independent Inflammation by Toll-like Receptor 4. Immunity 45: 46–59. [PubMed: 27396959]
49. Liu Q, Qiu J, Liang M, Golinski J, van Leyen K, Jung JE, You Z, Lo EH, Degterev A, and Whalen MJ. 2014. Akt and mTOR mediate programmed necrosis in neurons. Cell Death Dis 5: e1084. [PubMed: 24577082]
50. Knowles LM, Yang C, Osterman A, and Smith JW. 2008. Inhibition of fatty-acid synthase induces caspase-8-mediated tumor cell apoptosis by up-regulating DDIT4. J Biol Chem 283: 31378–31384. [PubMed: 18796435]
51. Villar VH, Nguyen TL, Delcroix V, Teres S, Bouchecareilh M, Salin B, Bodineau C, Vacher P, Priault M, Soubeyran P, and Duran RV. 2017. mTORC1 inhibition in cancer cells protects from glutaminolysis-mediated apoptosis during nutrient limitation. Nat Commun 8: 14124. [PubMed: 28112156]
52. Zhang DW, Shao J, Lin J, Zhang N, Lu BJ, Lin SC, Dong MQ, and Han J. 2009. RIP3, an energy metabolism regulator that switches TNF-induced cell death from apoptosis to necrosis. Science 325: 332–336. [PubMed: 19498109]
53. Moon JS, Hisata S, Park MA, DeNicola GM, Ryter SW, Nakahira K, and Choi AMK. 2015. mTORC1-Induced HK1-Dependent Glycolysis Regulates NLRP3 Inflammasome Activation. Cell Rep 12: 102–115. [PubMed: 26119735]
54. Lupfer C, Thomas PG, Anand PK, Vogel P, Milasta S, Martinez J, Huang G, Green M, Kundu M, Chi H, Xavier RJ, Green DR, Lamkanfi M, Dinarello CA, Doherty PC, and Kanneganti TD. 2013. Receptor interacting protein kinase 2-mediated mitophagy regulates inflammasome activation during virus infection. Nat Immunol 14: 480–488. [PubMed: 23525089]
55. Saavedra PHV, Huang L, Ghazavi F, Kourula S, Vanden Berghe T, Takahashi N, Vandenabeele P, and Lamkanfi M. 2018. Apoptosis of intestinal epithelial cells restricts Clostridium difficile infection in a model of pseudomembranous colitis. Nat Commun 9: 4846. [PubMed: 30451870]

KEY POINTS

1. RIPK3 promotes pyrin inflammasome activation independent of its role in necroptosis.
2. RIPK3 modulates the mTOR pathway to regulate pyrin inflammasome activation.
3. Inhibition of mTOR promotes *Mefv* expression and pyrin inflammasome activation.

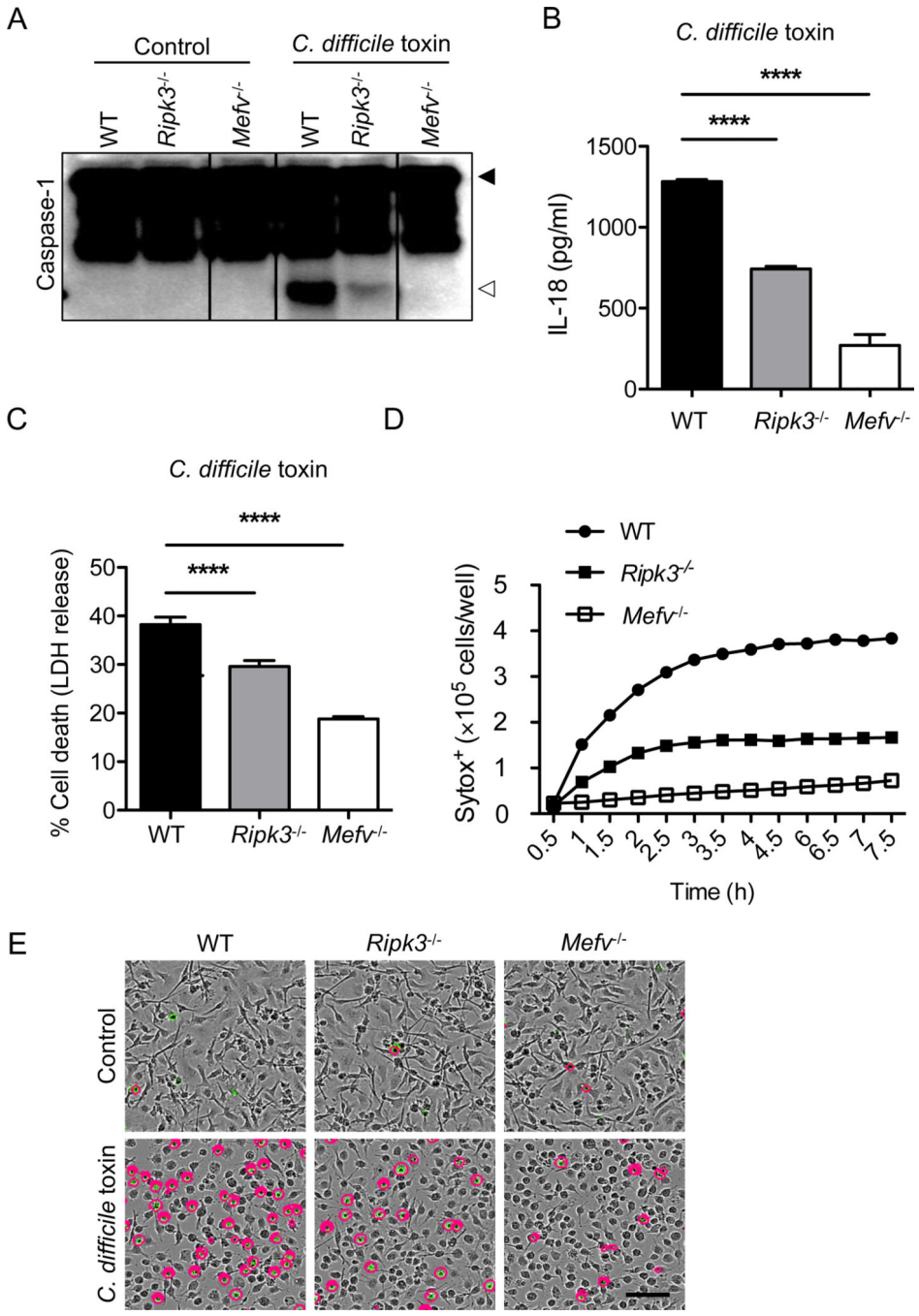

FIGURE 1. Role of RIPK3 in pyrin inflammasome activation.

(**A**) Immunoblot analysis of caspase-1 processing in bone marrow-derived macrophages (BMDMs) from wild type (WT) and knockout mice treated with control or *C. difficile* toxin stimuli for 6 hours. Filled arrow designates the pro-form (p45), and open arrow designates cleaved caspase-1 (p20). (**B**) IL-18 release after stimulation of BMDMs with control or *C. difficile* toxin stimuli for 6 hours. (**C**) Percent of BMDMs exhibiting membrane permeability after stimulation with control or *C. difficile* toxin stimuli for 6 hours, assessed by lactate dehydrogenase (LDH) release. (**D**) Number of BMDMs exhibiting membrane permeability

following stimulation with control or *C. difficile* toxin stimuli, assessed by Sytox staining. (**D**) Representative images of BMDMs stimulated with control or *C. difficile* toxin stimuli for 6 hours. The green demonstrates Sytox signal, and the pink mask outlines cells counted as dead in the analysis. Scale bar is 100 μM. Control refers to stimulation with supernatant from toxin-negative *C. difficile* cultures. Data are presented as mean ± s.e.m. (B and C) from technical replicates or as the average number from four fields of view (D), and data are representative of at least three independent repeats. ****$P < 0.0001$ using one-way ANOVA followed by Fischer's LSD post-test.

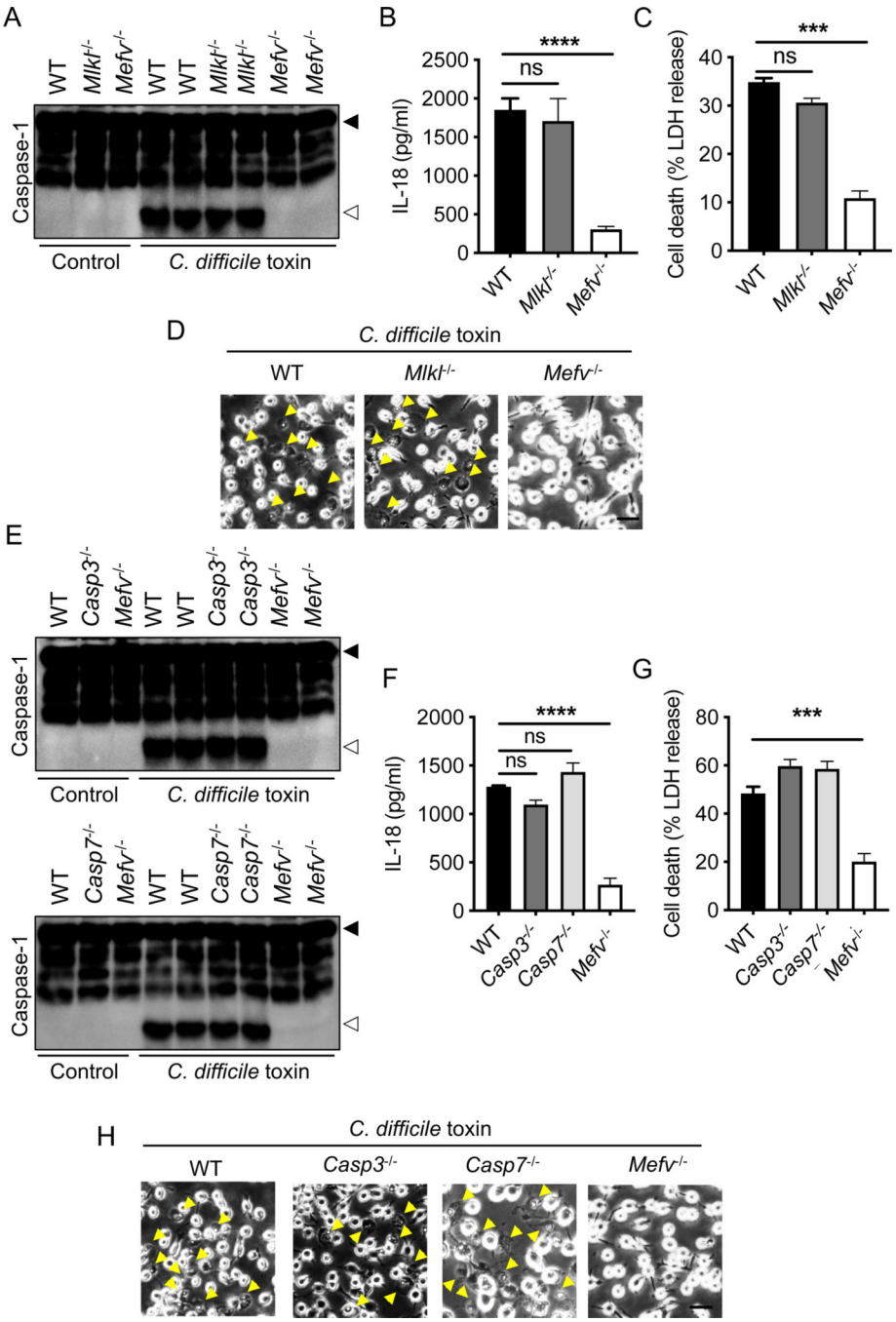

FIGURE 2. Activation of the pyrin inflammasome is independent of necroptosis.

(**A**, **E**) Immunoblot analysis of caspase-1 processing in bone marrow-derived macrophages (BMDMs) from wild type (WT) and knockout mice treated with control or *C. difficile* toxin stimuli for 6 hours. Filled arrow designates the pro-form (p45), and open arrow designates cleaved caspase-1 (p20). (**B**, **F**) IL-18 and (**C**, **G**) LDH release after stimulation of BMDMs with control or *C. difficile* toxin stimuli for 6 hours. (**D**, **H**) Representative images of BMDMs stimulated with control or *C. difficile* toxin stimuli for 6 hours obtained by brightfield microscopy. Blue arrows depict pyroptotic cell death. Scale bar is 20 μM. Control

refers to stimulation with supernatant from toxin-negative *C. difficile* cultures. Data are presented as mean ± s.e.m. (B, E, and H) from technical replicates, and are representative of at least three independent repeats. ns, not significant; ****$P < 0.0001$ using one-way ANOVA followed by Fischer's LSD post-test.

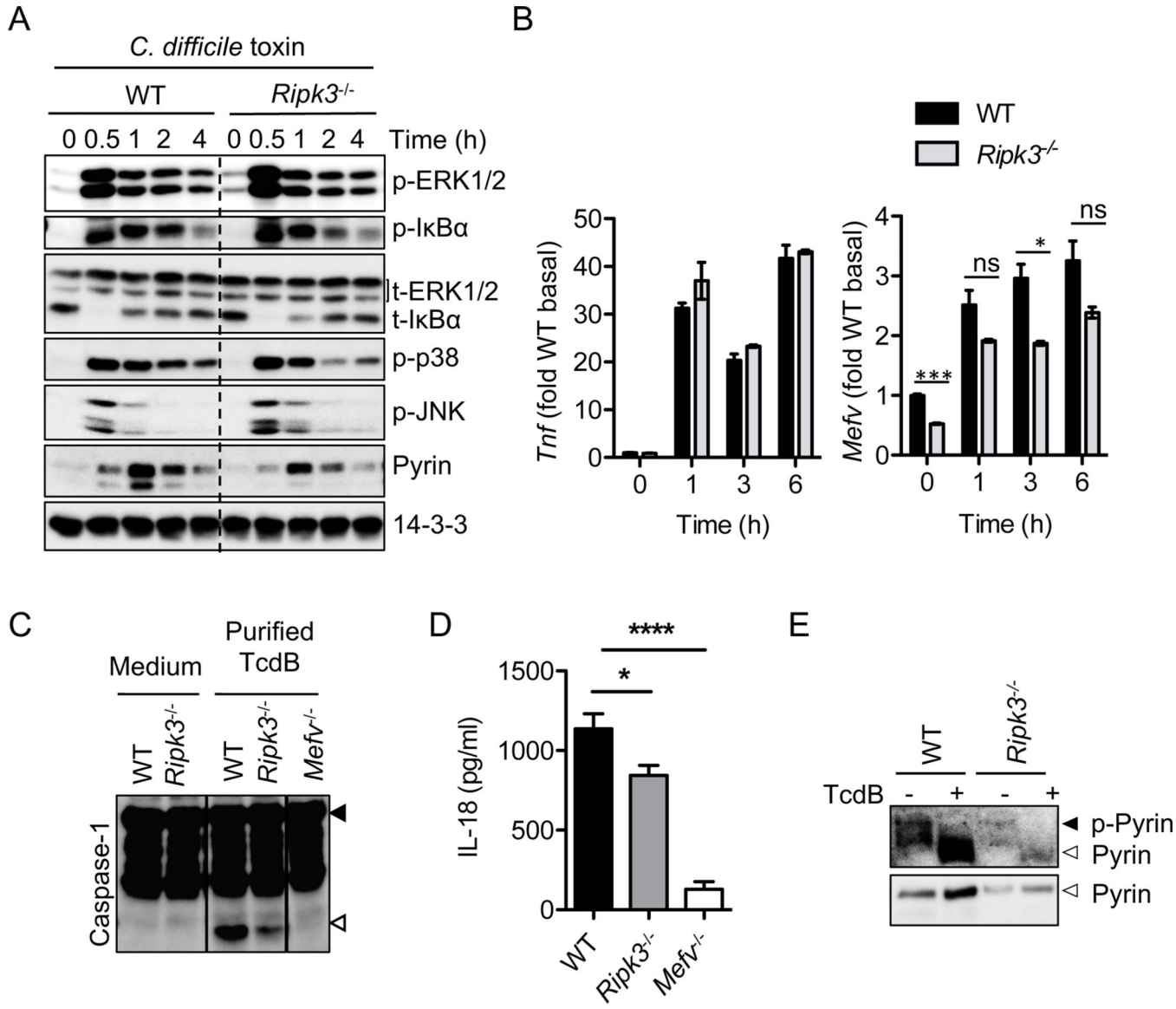

FIGURE 3. RIPK3 modulates pyrin inflammasome activation independent of inflammatory signaling or pyrin dephosphorylation.

(**A**) Immunoblot analysis of the activation status of MAPK and NF-κB pathways in bone marrow-derived macrophages (BMDMs) from wild type (WT) and knockout mice. (**B**) *Tnf* and *Pyrin* induction in BMDMs stimulated with control or *C. difficile* toxin stimuli. Expression was normalized to set WT expression at baseline to 1. (**C**) Immunoblot analysis of caspase-1 processing in BMDMs treated with or without purified *C. difficile* toxin B (TcdB) for 6 hours. Filled arrow designates the pro-form (p45), and open arrow designates cleaved caspase-1 (p20). (**D**) IL-18 release after stimulation of BMDMs with TcdB for 6 hours. (**E**) Immunoblot analysis of pyrin dephosphorylation in response to TcdB. The top panel shows the phos-tag gel, and the bottom panel shows the western blot probed with anti-pyrin antibody. An increase in migration (shown as the lower band) on a phos-tag gel depicts dephosphorylation of pyrin. Data are presented as mean ± s.e.m. (B, D) from technical replicates, and are representative of at least three independent repeats. ns, not

significant; *$P < 0.05$; ***$P < 0.001$; and ****$P < 0.0001$ using one-way ANOVA followed by Fischer's LSD post-test.

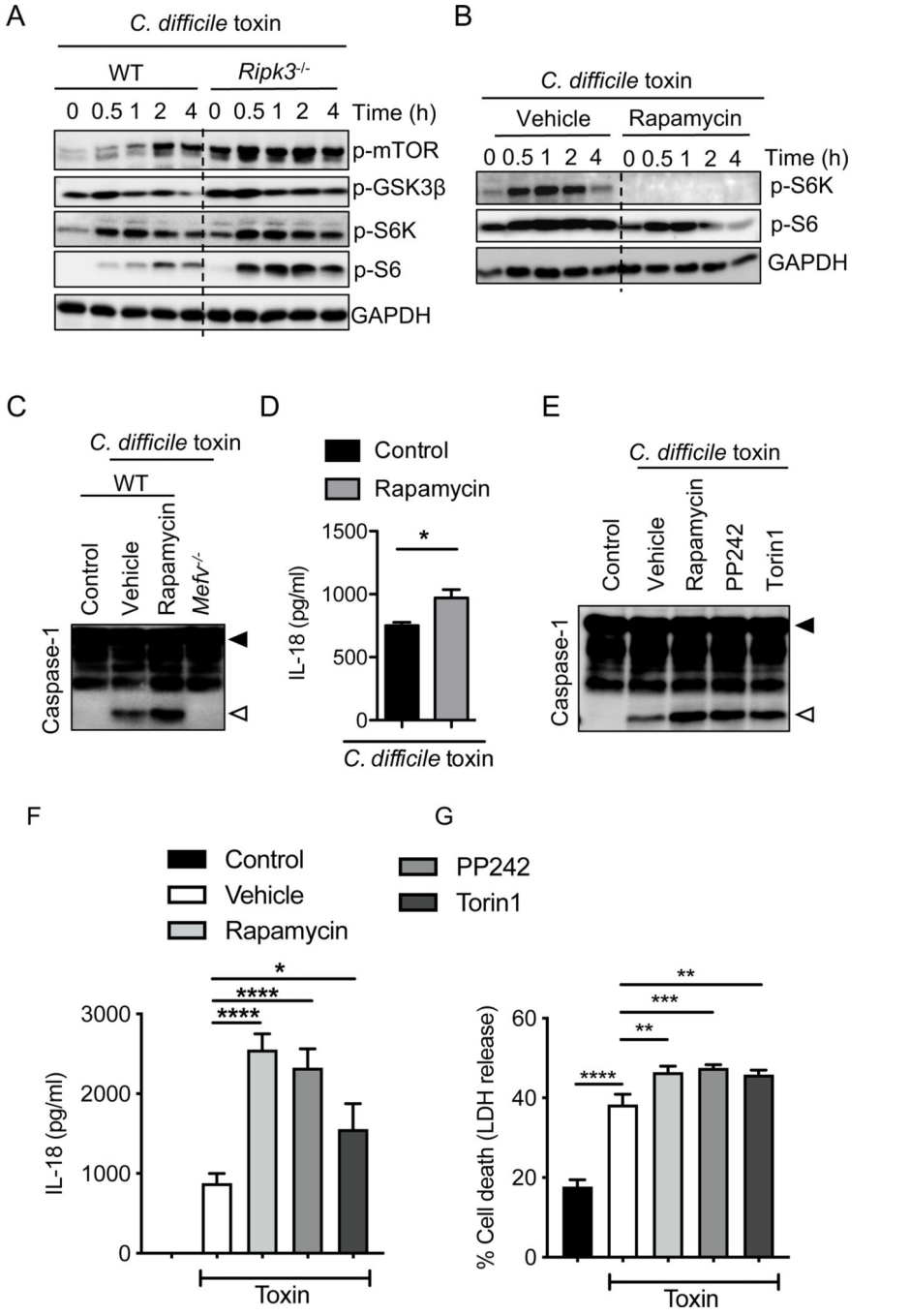

FIGURE 4. RIPK3 modulates pyrin inflammasome activation via mTOR signaling in response to *C. difficile* toxin stimuli.

(**A** and **B**) Immunoblot analysis of the activation status of mTOR and its downstream pathway in wild type (WT) and knockout (A) or WT (B) bone marrow-derived macrophages (BMDMs) stimulated with control or *C. difficile* toxin stimuli for the indicated time. (**C** and **E**) Immunoblot analysis of caspase-1 processing in BMDMs from WT or knockout mice treated with control or *C. difficile* toxin stimuli and either vehicle, rapamycin, PP242, or torin1 for 6 hours. Filled arrow designates the pro-form (p45), and open arrow designates

cleaved caspase-1 (p20). (**D** and **F**) IL-18 release after stimulation of WT BMDMs with control or *C. difficile* toxin stimuli for 6 hours. (**G**) Percent of BMDMs exhibiting membrane permeability after stimulation with control or *C. difficile* toxin stimuli for 6 hours, assessed by lactate dehydrogenase (LDH) release. (B–G) BMDMs were incubated with mTOR inhibitors rapamycin, PP242, or torin1 (as indicated) for 30 minutes prior to addition of control or *C. difficile* toxin stimuli. Control refers to stimulation with supernatant from toxin-negative *C. difficile* cultures. Data are presented as mean ± s.e.m. (D, F, and G) from technical replicates, and are representative of at least three independent repeats. $*P < 0.05$; $**P < 0.01$; $***P < 0.001$; and $****P < 0.0001$ using student's t-test (D and F) and one-way ANOVA followed by Fischer's LSD post-test (G).

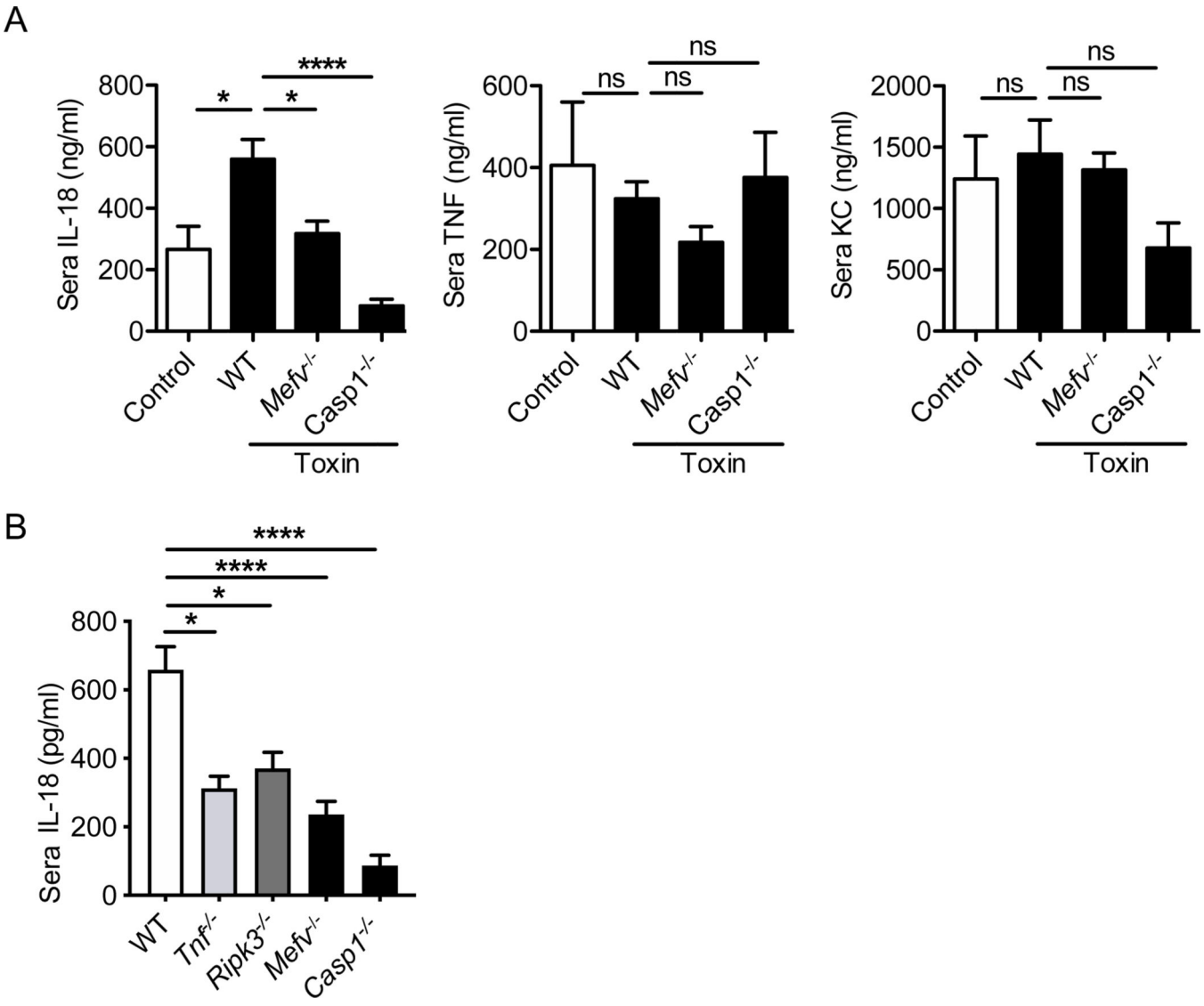

FIGURE 5: RIPK3 is required for pyrin inflammasome activation in vivo.

(**A**) Cytokine levels in the sera of wild type (WT) or knockout mice 4 hours post-intraperitoneal injection with supernatant from toxin-negative (control) or toxin-positive *C. difficile* cultures. (**B**) Cytokine levels in the sera of WT or knockout mice 4 hours post-intraperitoneal injection with supernatant from toxin-positive *C. difficile* cultures. Control refers to stimulation with supernatant from toxin-negative *C. difficile* cultures. Data are pooled from two to three independent repeats, and N = 7–15 for each genotype. ns, not significant; $*P < 0.05$; and $****P < 0.0001$ using one-way ANOVA followed by Fischer's LSD post-test or Kruskal-Wallis and Dunn's post-test.